# Direct observation of the spin-dependent Peltier effect

Flipse, J.; Bakker, F. L.; Slachter, A.; Dejene, F. K.; van Wees, B. J.

*Published in:*
Nature Nanotechnology

*DOI:*
10.1038/NNANO.2012.2



*Publication date:*
2012

nature nanotechnology

SUPPLEMENTARY INFORMATION

DOI: 10.1038/NNANO.2012.2

# Direct observation of the spin-dependent Peltier effect

J. Flipse, F. L. Bakker, A. Slachter, F. K. Dejene & B. J. van Wees

## A. Calculation of the temperature gradient

We first derive an expression for the Peltier coefficient of the separate spin channels $\Pi_{\uparrow,\downarrow}$ in terms of the conventional Peltier coefficient $\Pi$ and the conductivity polarization $P_\sigma = \frac{\sigma_\uparrow - \sigma_\downarrow}{\sigma_\uparrow + \sigma_\downarrow}$.

In the bulk of the ferromagnet $\nabla\mu_\uparrow = \nabla\mu_\downarrow = \nabla\mu_C$ and the Peltier heat current can be written as the sum of that of the separate spin channels, $-\Pi_\uparrow\sigma_\uparrow\nabla\mu_\uparrow - \Pi_\downarrow\sigma_\downarrow\nabla\mu_\downarrow = -\Pi\sigma\nabla\mu_C$, where we use $J_C = -\sigma\nabla\mu_C$ and $J_{\uparrow,\downarrow} = -\sigma_{\uparrow,\downarrow}\nabla\mu_{\uparrow,\downarrow}$ as the definitions of the electrochemical potentials $\mu_C$ and $\mu_{\uparrow,\downarrow}$. Using the spin-dependent conductivities $\sigma_{\uparrow,\downarrow} = \frac{\sigma}{2}(1 \pm P_\sigma)$, we obtain $\Pi = \frac{\sigma_\uparrow\Pi_\uparrow + \sigma_\downarrow\Pi_\downarrow}{\sigma}$.

Rewriting the result gives us the relation for the Peltier coefficients for majority and minority electrons:

$$\Pi_{\uparrow,\downarrow} = \Pi - \frac{1}{2}(P_\sigma \mp 1)\Pi_S \qquad (1)$$

where we define $\Pi_S = \Pi_\uparrow - \Pi_\downarrow$ as the spin-dependent Peltier coefficient.

Next, we derive an expression for the temperature gradient that develops in the ferromagnetic region for the general case when a spin current is accompanied by a charge current $J_C = J_\uparrow + J_\downarrow$. The Peltier heat current is given by $Q_\Pi = \Pi_\uparrow J_\uparrow + \Pi_\downarrow J_\downarrow$ and the temperature gradient is calculated by considering the total heat current in the ferromagnet $Q = Q_\Pi - \kappa\nabla T$, where $\kappa$

DOI: 10.1038/NNANO.2012.2

describes the thermal conductivity of the electron and phonon system. For simplicity, we assume that no heat can enter or leave the stack (Q = 0) and disregard Joule heating. Then we can write $\nabla T = -\frac{1}{\kappa}[\Pi_{\uparrow}\sigma_{\uparrow}\nabla\mu_{\uparrow} + \Pi_{\downarrow}\sigma_{\downarrow}\nabla\mu_{\downarrow}]$ and from the definition of the spin-dependent conductivity and the Peltier coefficients for majority and minority electrons, we find:

$$\nabla T = -\frac{\sigma}{\kappa}\left(\Pi\nabla\mu_C + \frac{1}{4}(1-P_{\sigma}^2)\Pi_S\nabla\mu_S\right) \qquad (2)$$

with $\Pi$ is the charge Peltier coefficient and $\mu_S = \mu_{\uparrow} - \mu_{\downarrow}$ the spin accumulation. The electrochemical potential is here derived from current conservation $J_C = J_{\uparrow} + J_{\downarrow} = -\sigma\nabla\mu_C$ and by substitution of $J_{\uparrow,\downarrow}$ with $-\sigma_{\uparrow,\downarrow}\nabla\mu_{\uparrow,\downarrow}$, we write $\nabla\mu_C = \frac{\sigma_{\uparrow}\nabla\mu_{\uparrow} + \sigma_{\downarrow}\nabla\mu_{\downarrow}}{\sigma}$.

The first term of Eq. 2 describes the conventional Peltier effect in the absence of spin accumulation. The second term describes what happens if a spin accumulation is present in the ferromagnet. According to Eq. 2, this gives rise to an additional temperature gradient which depends exclusively on the gradient of the spin accumulation in the ferromagnetic layer and is therefore magnetically controllable. Since spin relaxation forces the spin accumulation to decrease exponentially in the ferromagnetic region[24], we can write $\mu_S = \mu_S^0 \exp(-x/\lambda_F)$ with $\lambda_F$ the spin relaxation length. The conventional Peltier term leads to a constant temperature gradient independent of the spin accumulation. By integrating only the spin-dependent Peltier term of Eq. 2, we obtain a temperature difference between the F/N interface and the bulk of the ferromagnet of:

$$\Delta T = \frac{\sigma}{4\kappa}(1-P_{\sigma}^2)\,\Pi_S\mu_S^0 \qquad (3)$$

where $\mu_S^0$ is the spin accumulation at the interface. Here we find that the induced temperature drop depends directly on the spin accumulation at the F/N interface.

## B. Electrochemical potential profile extracted from the modeling

In the temperature profile we obtain from the modeling, the small temperature change due to the spin-dependent Peltier effect is not visible as the much larger Joule heating and (charge Peltier) heating disguise it. For this reason we do not show the temperature profile here. In Supplementary Figure 1 below, the modeling results of the electrochemical potential for the individual spin channels are shown.

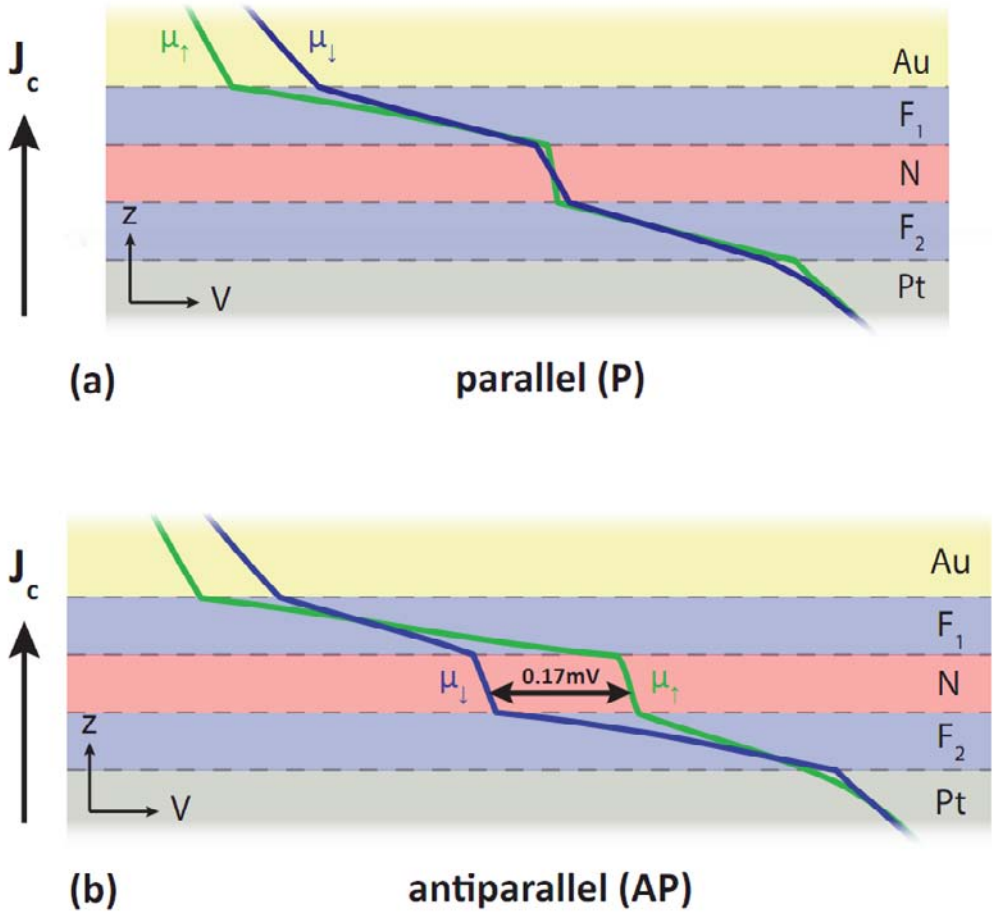


**Supplementary Figure 1 Spin electrochemical potentials extracted from the modeling.** The spin electrochemical potentials throughout the stack for the parallel (P) and anti-parallel (AP) configuration of the ferromagnets as given by the modeling (rms current of 1 mA). Going from the P to AP configuration the magnetization of the $F_2$ layer is reversed. **a,** parallel configuration. **b,** antiparallel configuration.

DOI: 10.1038/NNANO.2012.2

## C. Second harmonic response (Joule heating)

The second harmonic response signal (see Supplementary Fig. 2) originates from Joule heating in the device and is proportional to $I^2 R$. This dependence on R causes a change in Joule heating[17,19] when the resistance of the spin valve stack changes from the P to AP configuration and vice versa. Changes in Joule heating in the spin valve stack are picked up by the thermocouple and show up in the second harmonic response measurement, $R_{3-4}^{(2f)}$, as they depend on $I^2$. In our model we explicitly take in to account the heat generation due to energy dissipation related to spin relaxation[21]. From the model we then obtain the background and spin signal, which are approximately two times higher than observed in the measurement. We explain this by inefficiency in the temperature sensing, owing to the discrepancy between modeling parameters and the actual, experimental values. Moreover, a big part of the background Joule heating takes place in the Pt bottom contact. The cross linked PMMA, not included in the modeling, covers this contact thereby lowering the background Joule heating signal.

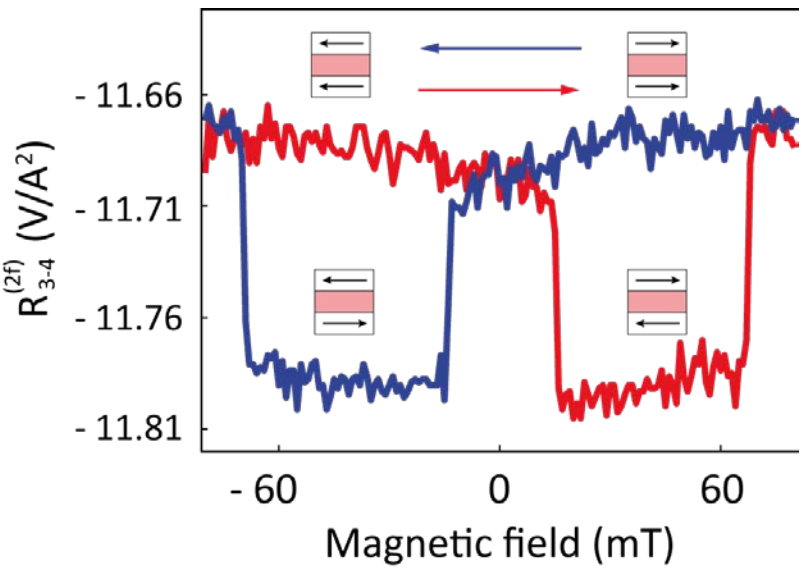


**Supplementary Figure 2 Joule heating measurement.** Second-harmonic response signal, $R_{3-4}^{(2f)} \equiv V_{3-4}^{(2f)} / I^2$, measured at the thermocouple with a root mean square current of 1mA.

## D. Results for two other samples

The spin-dependent Peltier measurements were performed on two other samples of the same batch and are presented in Supplementary Fig. 3. The first sample (Supplementary Fig. 3a) shows a spin-dependent Peltier signal of –100 μΩ on a background of –0.55 mΩ and the second (Supplementary Fig. 3b) a –110 μΩ spin-dependent Peltier signal on a –0.56 mΩ background. These values are somewhat higher than for the sample discussed in the main text. The observed variation can be attributed to a slightly higher efficiency of the thermocouple of these samples and/or small differences in thermal anchoring, aluminum oxide thickness and lithographic alignment. The switching that is observed prior to sweeping through zero field is due to interaction between the magnetic dipole fields of the two Py layers, which favors an AP alignment. The sample to sample variation of the switching field position has been seen in several batches for different experiments and can be attributed to for instance small variations in cross section of the pillar. Extracting the spin-dependent Peltier coefficient from this data in the same way as discussed in the main text gives values for $\Pi_S$ of –1.1 and –1.3 mV.

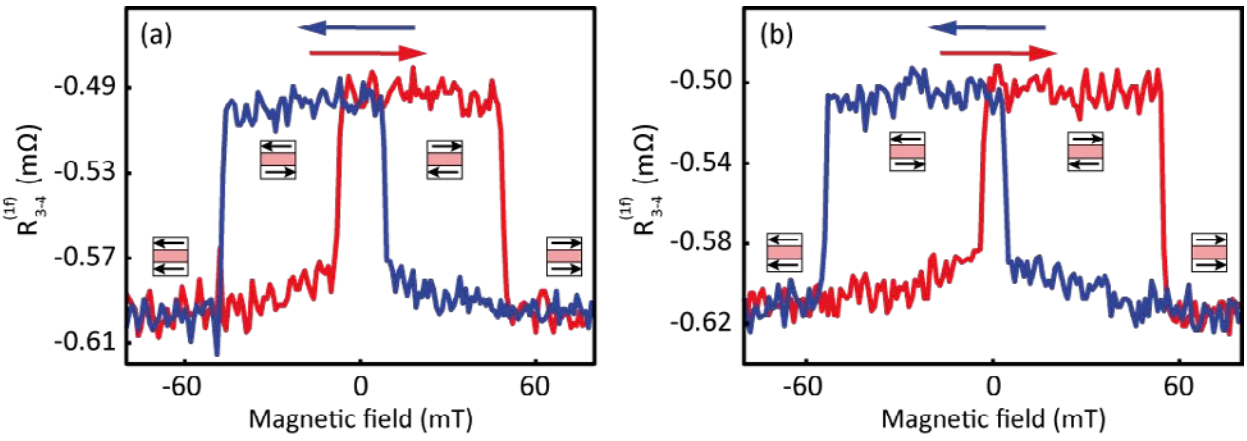


**Supplementary Figure 3 Spin-dependent Peltier measurements for two other samples.** First-harmonic response signal, $R_{3-4}^{(1f)} \equiv V_{3-4}^{(1f)} / I$, measured at the thermocouple with a root mean square current of 1 mA. In **a** the results for sample 2 are shown and in **b** those for sample 3.

DOI: 10.1038/NNANO.2012.2

## E. Measurements at 77K

The presented measurements were repeated on the same sample at liquid nitrogen temperature (77K). This was done to confirm that the first harmonic spin signal is indeed caused by the spin dependency of the Py Peltier coefficient. From the Thomson-Onsager relation, $\Pi_{\uparrow,\downarrow} = T*S_{\uparrow,\downarrow}$, together with the fact that the Seebeck coefficient shows a dependency on temperature, it becomes clear that $\Pi_S$ (Supplementary A) and thereby the spin-dependent Peltier effect will decrease when lowering the temperature. The spin-dependent Peltier measurement at 77K is presented in Supplementary Fig. 4a and shows no difference between P and AP alignment. The disappearance of the spin signal at low temperature supports our conclusion that the room temperature spin signal can be attributed to the spin-dependent Peltier effect. At the same time the background signal, which originates from the conventional Peltier effect, remains almost the same. This can be explained by the fact that for the spin-dependent Peltier effect only the Peltier coefficient of Py plays a role whereas for the Peltier background the difference between all the Peltier coefficients in the current path are important. The Peltier coefficient is proportional to the Seebeck coefficient ($\Pi=S*T$) whose temperature dependence does not have to be the same for different materials. Together with a change in thermal conductance between different temperatures it is possible for the regular Peltier effect contribution to not show a decrease when going from room temperature to 77K.

The spin valve measurement shown in Supplementary Fig. 4c shows a decrease in background resistance due to an increase of the conductivities at lower temperatures. The bigger spin signal that is observed is caused by the spin relaxation lengths increasing with lowering of the temperature.

As the Joule heating depends on the resistance, the increase of the materials'

conductivities at 77K will give a lower second harmonic background signal, which is in accordance with the measurement shown in Supplementary Fig. 4b. At the same time the second harmonic spin signal goes up because of the increased difference in resistance between P and AP alignment shown in the spin valve measurements. In the measurement this increase is smaller due to temperature dependences of the Seebeck coefficients and thermal conductivities.

In conclusion we can say that the disappearance of the first harmonic signal, while the spin valve signal increases, rules out the possibility of it originating from spin valve voltage pick up and is consistent with the spin-dependent Peltier effect. Furthermore the second harmonic and spin valve measurement behavior confirm the lowering of the reference temperature and the correct operation of the device and thermocouple.

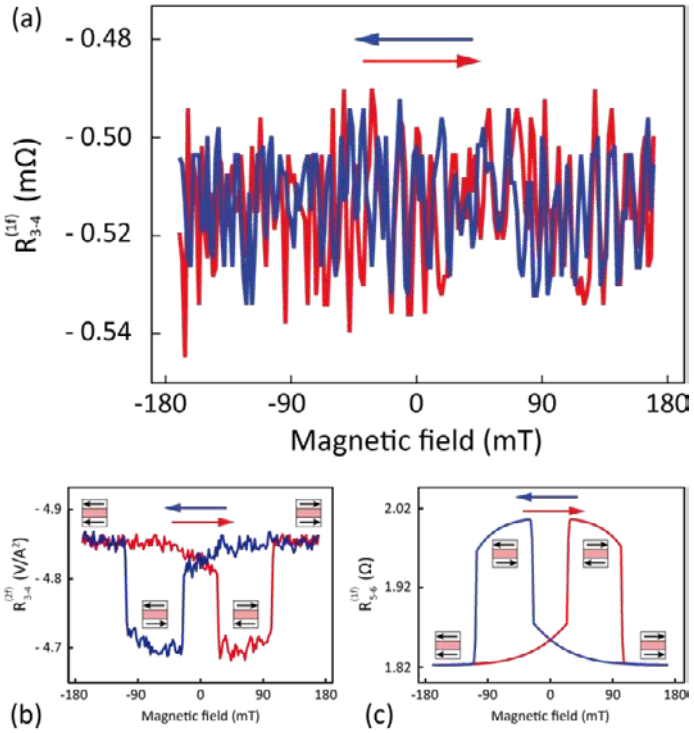


**Supplementary Figure 4 Measurements at 77K. a,** First-harmonic response signal, $R_{3-4}^{(1f)} \equiv V_{3-4}^{(1f)} / I$, at 77K measured at the thermocouple with a root mean square current of 1 mA. **b,** Second-harmonic response signal, $R_{3-4}^{(2f)} \equiv V_{3-4}^{(2f)} / I^2$, at 77K measured at the thermocouple with a root mean square current of 1 mA. **c,** Spin valve measurement at 77K on the same device.

DOI: 10.1038/NNANO.2012.2

## F. Modeling parameters

$T_0 = 300K$

| Material | $\sigma$ [S m$^{-1}$] | $\Pi$ [mV] | $\lambda$ [nm] | $\kappa$ [W m$^{-1}$ K$^{-1}$] |
|---|---|---|---|---|
| **Au** | $2.2 \times 10^{7}$ | 0.51 | 80 | 300 |
| **Pt** | $9.5 \times 10^{6}$ | -1.5* | 5 | 72 |
| **Cu** | $4.3 \times 10^{7}$ | 0.48 | 350 | 300 |
| **Py** | $4.3 \times 10^{6}$ | -6.0* | 5 | 30 |
| **NiCu** | $2.0 \times 10^{6}$ | -9.6* | 5 | 20 |
| **$SiO_2$** | $1.0 \times 10^{-13}$ | 0 | - | 1 |
| **$Al_2O_3$** | $1.0 \times 10^{-13}$ | 0 | - | 30 |

**Supplementary Table 1 Input parameters for the modeling**.

* The Peltier coefficient was determined in a separate device specifically designed to accurately determine the Seebeck/Peltier coefficient of a material.

References:

24. Valet, T. & Fert, A. Theory of the perpendicular magnetoresistance in magnetic multilayers. *Phys. Rev. B* **48**, 7099–7113 (1993).